Jurnal Penelitian Fisika dan Aplikasinya (JPFA) *Volume 10, Issue 02, December 2020*
p-ISSN: 2087-9946 DOI: 10.26740/jpfa.v10n2.p137-145
e-ISSN: 2477-1775 https://journal.unesa.ac.id/index.php/jpfa

Research Article

Reconstruction of High Resolution Medical Image Using General Regression Neural Network (GRNN)

Yudha Satya Perkasa [1,a], Khoerun Nisa Syaja'ah [1,b,*], Lyana Ismadelani [1,c], and Rena Denya Agustina [2,d]

[1] Department of Physics, Faculty of Science & Technology, Universitas Islam Negeri Sunan Gunung Djati Bandung
Jalan A.H. Nasution No. 105, Bandung 40614, Indonesia
[2] Department of Physics Education, Faculty of Education, Universitas Islam Negeri Sunan Gunung Djati Bandung
Jalan A.H. Nasution No. 105, Bandung 40614, Indonesia

e-mail: [a] yudha@uinsgd.ac.id, [b] nisasya@uinsgd.ac.id, [c] ismadelanilyana@gmail.com, and [d] renadenya@uinsgd.ac.id
* Corresponding Author

Abstract

Low image resolution has deficiencies in the diagnostic process, this will affect the quality of the image in describing an object in certain tissues or organs, especially in the process of examining patients by doctors or physicians based on the results of imaging medical devices such as CT-scans, MRIs and X-rays. Therefore, this study had developed a General Regression Neural Network (GRNN) type artificial neural network system to reconstruct a medical image so that the image has a significant resolution for the analysis process. The GRNN input layer uses grayscale intensity values with variations in the image position coordinates to produce an optimal resolution. There are four layers in this method, the first is input layer, the second is hidden layer, the third is summation, and the last layer is output. We examined the two parameters with different interval values of 0.2 and of 0.5. The result shows that the interval value of 0.2 is the optimal value to produce an output image that is identical to the input image. This is also supported by the results of the intensity curve of the RGB pattern matched between target and output.

Keywords: *General Reconstruction Neural Network; Resolution; Interval; Medical image; Reconstruction*

Rekonstruksi Citra Medis Resolusi Tinggi Menggunakan General Regression Neural Network (GRNN)

Abstrak

Resolusi gambar yang rendah memiliki kekurangan dalam proses diagnosa hal ini akan mempengaruhi kualitas citra dalam menjelaskan sebuah objek pada jaringan atau organ tertentu terutama pada proses pemeriksaan dokter berdasarkan hasil pencitraan alat medis seperti CT-scan, MRI, X-ray. Oleh karena itu, penelitian ini mengembangkan sistem jaringan syaraf tiruan tipe GRNN untuk melakukan rekonstruksi citra medis agar citra tersebut memiliki resolusi yang cukup signifikan bagi proses analisis selanjutnya. Lapisan input GRNN menggunakan nilai intensitas grayscale dengan variasi interval posisi

koordinat citra untuk menghasilkan optimasi rekonstruksi resolusi. terdapat 4 lapisan dalam perhitungan GRNN yang pertama adalah lapisan input, yang kedua dan ketiga adalah lapisan tersembunyi dan kelas atau gabungan dan yang terakhir adalah lapisan output. kami menggunakan dua nilai interval parameter yaitu dengan nilai 0.2 dan 0,5. Hasil perhitungan menunjukkan bahwa nilai interval 0,2 merupakan nilai optimal untuk menghasilkan citra output yang identik dengan citra input. Hal ini didukung pula dengan hasil kurva intensitas terhadap posisi koordinat dari perbandingan kurva RGB. Kurva RGB merupakan perbandingan dari citra yang dijadikan target dan hasil simulasi. dari hasil tersebut didapat kecocokan pola pada koordinat yang sama.
Kata Kunci: *General Reconstruction Neural Network, Resolusi, Interval, Citra medis, Rekonstruksi*

PACS: 85.57.-s; 87.57.Ce; 87.85.dq; 87.57.Nk; 42.30.Wb

Article History: Received: December 12, 2019 Aproved with minor revision: December 4, 2020
Accepted: December 26, 2020 Published: December 31, 2020

How to cite: Perkasa Y S, et al. Reconstruction of High Resolution Medical Image Using General Regression Neural Network (GRNN). *Jurnal Penelitian Fisika dan Aplikasinya (JPFA)*. 2020; **10**(2): 137-145. DOI: https://doi.org/10.26740/jpfa.v10n2.p137-145.

I. INTRODUCTION

X-rays beam is created from interaction of matter of atomic level in electron shells [1]. There are three main processes: photoelectric effect, Compton scattering, and pair production [2]. The interaction occurs in the region of high electron density based on photons and electrons [3].

X-ray attenuation is the effect of the interaction between matter and the photon during the photoelectric or Compton effect, in which some photons will pass through matter or tissue in the human body [4]. During every projection, the indicator signals give data about the absolute tissue attenuation between the source and detector [5,6]. High resolution CT requires high density samples [6]. In the event that a lacking number of projections are taken, streaking is seen [7].

The axial spatial resolution is primarily controlled by the separations between the X-beam tube, the focal point of revolution [8], the detector functioning as the width of the focus, and the detector elements, as well as the quantity of estimations made per rotation. Absorption signal that have been gathered as single dimensional qualities should now be shown as a two-dimensional picture.

Resolution on digital imaging has been highly beneficial for output medical equipment such as dental practice, X-ray machine, and CT-scan. In comparison to conventional radiological film-based, digital imaging needs less time preparation while provides more comfortable stream to share the result to the patient to describe a diagnostic result [8, 9, 10]. On the other hand, digital image resolution is the best reason for failures in proper printing or digitizing such as zoom in and zoom out. Its process can provide some artifacts that should be prevented [9,10].

Digital image processing is one of the manipulation tools using a computer algorithm or code to represent image [11]. Medical image processing for diagnosis is done through two general steps, namely preprocessing and post-processing. The results of post-processing are determined by the quality of pre-processing [12,13]. Pre-processing stage includes filtering [13], transformation, morphology, and thresholding. The purpose of filtering is to produce noise from medical images properties while transformation is aimed to create the clarity of the image [14,15]. While morphology is used to change the image for post-processing kernel matrix, thresholding is used to produce binary images [16,17]. The pre-processing method is very dependent on the quality of the resolution of the analyzed image. If the image resolution is very low [18,19], the result will have poor accuracy in the image analysis [20,21,22].

Panda, *et al* [23] found that image compression using BPNN (Back engendering neural organization) is an effective process of coding a computerized picture, to minimize the number of bits required in describing the image. Its aim is to enable good quality of produced images. Besides, Ahmad Jobran Al-Mahasneh *et al* [24] describe about the differences between GRNN (Generalized Regression Neural Network) and BPNN from each algorithm and function. First, GRNN is a single-pass learning algorithm, while BPNN needs two passes: forward and backward pass. It can be concluded that GRNN has significantly fewer training time. Second, the only free parameter in GRNN is the smoothing parameter, this also shows that GRNN has the quick learning and easy to use for online systems because only minimal computations are required.

Meanwhile the reconstruction of image resolution based on the GRNN had never been conducted. Therefore, it is necessary to develop a method for reconstructing medical images in order to have a better image resolution. In this research, an image reconstruction method was developed using a GRNN neural network through input data modelling processes that have good resolution with minimum error limit. Furthermore, the Artificial Neural Network (ANN) system will be used to improve the medical image resolution using different interval values of the coordinate system. Hopefully, the optimal value of coordinate interval could be obtained for better image resolution.

II. METHOD

The method consists of two main parts of the experiment: the first is input and reading file RGB, and the second is determining the parameter and target using GRNN including simulation of the neural network process.

Input and Reading File

Image samples used as input in the system are medical images with *.jpg, *. bmp, or *.png format. The sample used in this research is a medical image with low resolution of 100 × 100 pixels. The system will read automatically the image pixels at each coordinate point of the medical image. The input image in this system will be represented as an RGB matrix (Red Green Blue), the coordinates of the point (pixels) of the image, and its intensity value. This intensity value is resulted from the thresholding process in order to obtain binary image (grayscale). The order of the matrix is obtained from x and y coordinate value of the image and the matrix component is obtained from the grayscale intensity value as figure 1.

$$\begin{pmatrix} I_{11} & I_{12} & \cdots & I_{1y} \\ I_{21} & I_{22} & \cdots & I_{2y} \\ I_{31} & I_{32} & \cdots & \cdots \\ I_{41} & I_{42} & \cdots & I_{xy} \end{pmatrix}$$

Figure 1. The Matrix Intensity of Pixel

Aside from the RGB value, the data would be extracted as the process reaches the final stage so we can compare the RGB target pattern and the value to the resulting image that we are simulating

GRNN Simulation Process

GRNN uses input data in the form of a grayscale matrix or an RGB matrix. The order of the input matrix is determined by the interval (spacing) of the x and y coordinates. This interval will directly affect the resolution of the output image. A small number of interval will produce a large output image resolution. A small interval will also affect the number of neurons in the input layer. Thus, the number of intervals will be varied to determine the optimum interval value that could produce images with good resolution.

Figure 2 presents the scheme layer of GRNN. The input layer consists of input neurons which function is to receive information. These neurons will get an initial predictor value that will be used for the regression data. Hidden neurons get a predictor value of all the neurons present in the input layer. All predictors score this distribution. GRNN is derived from forward feedback artificial neural networks that are developed using radial basis function. In detail, GRNN has a transfer function in the form of gaussian function $\exp\left(-\frac{D_j^2}{2}\sigma^2\right)$ that is generated from the initial input distribution equation (Equation 1).

$$D_i^2 = (X - X_i)T.(X - X_i) \quad (1)$$

In the summation layer, there are two neurons with different functions. The first neuron functions to produce the denominator, while the second neuron functions to generate a numerator by adding the product of the weights on class and output layers. The last layer is the decision layer. In this layer, the accumulated numerator results will be divided by the accumulated denominator results so that it will produce a norm product. The output layer is the combination of calculation training process from the simulation network of each neuron. The GRNN diagram will automatically started from the first layer if the output does not match with the target.

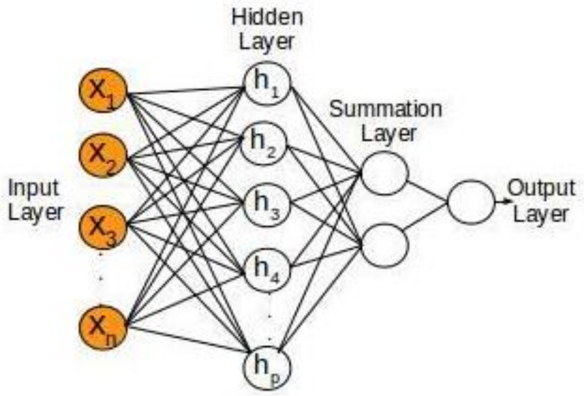

Figure 2. The Scheme Layer of GRNN

GRNN used to create radial distribution from input data using the gaussian function as an approximated function. This gaussian function is also used in inter-layer transfer. Smallest error approximation (MSE) is developed using input data with respect to target data. This should have been done using one of the common methods in neural networks.

The MSE optimization process uses the Levenberg-Marquardt algorithm in MATLAB which in principle optimizes the objective function using equation (2) and equation (3). This equation is a developed Backpropagation algorithm which makes improvements to speed up the network training process with numerical optimization techniques.

$$\begin{aligned} F(x) &= \frac{1}{2}\Sigma_{i=1}^{m}(f_i(x))^2 \\ &= \frac{1}{2}\| f(x)_2^2 \| \\ &= \frac{1}{2}f(x)^T f(x) \end{aligned} \quad (2)$$

$$\begin{aligned} \nabla F(x) &= F'(x) \\ &= \left(\frac{\delta F}{\delta x_i}(X)\ldots\frac{\delta F}{\delta x_n}(X)\right) \\ &= \left(\Sigma f_i(x)\frac{\delta f_i}{\delta x_i}(x)\ldots\Sigma f_i(x)\frac{\delta f_i}{\delta x_n}(x)\right) \\ &= J(x)^T f(x) \end{aligned} \quad (3)$$

III. RESULTS AND DISCUSSION

Figure 3 shows the medical images used in this research, which is the x-ray image of normal human legs with resolution of 100 × 100 px. Figure 3(a) is the 100 x 100 px image which is used as target on this experiment, and figure 3(b) is the same image with lower resolution that is used as input data to the GRNN process. As seen, the GRNN input picture was unclear. We try to train this object to get the new result as a good image as visual and get better resolution.

Figure 3. (a)The Target, and (b) Input Picture

Figure 4 shows the result of the parameter interval value (0.5) having been produced as an output image with resolution of 200 × 200. The medical image of the network simulation result is quite close to the target medical image but the medical image produced in this test is not broken but blurry. Meanwhile, in Figure 5 it is shown that the GRNN result for the lowest interval value of 0,2 could obtain a 500 × 500 px output image with a better resolution. The quality of image resolution that resulted from GRNN could be also determined using the curve of pixel intensity in the image coordinate system. In addition, the quality of image resolution that resulted from GRNN could also be determined using the curve of pixel intensity in the image coordinate system as shown in Figure 6.

The Figure 6 presents the RGB value intensity of pixels for target and result of GRNN with interval value of 0.2. The target values are represented with the line black color, while the RGB from the output file is shown in Red Green Blue coordinate intensity. Simulation results are at coordinates x, y = 0 to 245,025. Since the target R, G, B values and simulation results are at the same coordinates, it can be seen that the pattern generated by the network coincides with the pattern of that the network targets. It indicates the results of simulation are close to target value. Patterns generated by the R, G, B target values and values R, G, B network simulation results are different. This is due to the initialization of random weights on the Backpropagation network.

Figure 4. (a) The Target Medical Imaging, (b) Picture Input and (c) Output as Result of GRNN with Interval Value 0.5

Figure 5.(a) The Target Medical Imaging, (b). Picture Input and (c). Output as Result of GRNN with Interval Value 0.2

The GRNN system is also tested for several interval values, that is of 0.5 and of 0.2. The results of the curves show that the output image (with color) has better agreement with the target image intensity value comparison of the R, G, B values 0.2 of the network simulation results as shown in Figure 6. Results from smaller interval values had shown better approximation than the other values. It is because the large amount of data input will determine a better approximation model in GRNN. This is due to the large amount of GRNN input data compared to the previous results [25-30]. However, the large amount of input data could increase the computational time [23-24, 29-30].

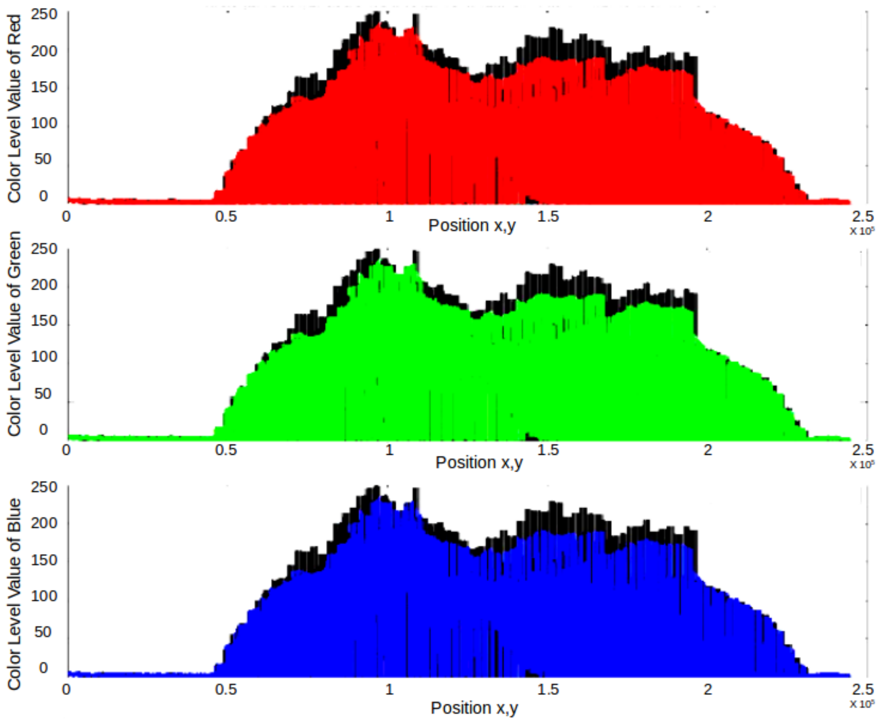

Figure 6. The Intensity Curve Value of Point Pixels to Coordinate Position Pixels for Interval Value 0.2

Alilouo *et al* describe GRNN networks are rapid at converging to the optimal regression surfaces using only some number of information samples. They also imitate the behavior of real biological neurons and are capable of approximating any complex or simple function [23]. Our results agree with this finding, it is related with the result shown in Figure 4 and Figure 5. The experiment of Panda *et al* [24] also described that GRNN has good performance in the result of image compression, in which they find and analyze for different images including X-ray device, Ultrasonography (USG) and Magnetic Resonance Imaging (MRI) [25-27, 30].

One of the advantages of GRNN that emerge in this research is the number of neurons in the hidden layer and the final layer does not change even though the amount of data is getting bigger [28-30]. It will only affect the iteration time of the Levenberg-Marquardt optimization process. Further improvement could be implemented using other forms of neural networks such as the modified backpropagation networks. This type of neural network is used to predict different images compared to input data. It could also use a quantitative method such as SNR (signal to noise ratio) to measure the noise ratio in the images.

CONCLUSION

We successfully developed the GRNN method to make a good resolution for medical imaging purposes. This image was processed by determining the target, so the input picture can be trained, producing best resolution and can represent the image without reducing the information. The best result is shown by the use of the lowest interval value of 0.2, in which GRNN could obtain a 500 x 500 px output image with a better resolution. This is evidenced by plotting the RGB curve of the target image with the GRNN results that are close to the target value.

The GRNN neural network uses input data to create approximated functions related to image intensity. This model of function could be better calculated using enormous amounts of input data. However, this also could lead to an increase in computation time. This enormous input data could be obtained by minimizing interval coordinate in the images.

ACKNOWLEDGMENT

This research is supported by Daftar Isian Pelaksana Anggaran (DIPA) Lembaga Penelitian dan Pengembangan Kepada Masyarakat (LP2M), 2017 of Universitas Islam Negeri (UIN) Sunan Gunung Djati Bandung, with contract number B-346/B.2-006/Un.05/V.2.PP.00.9/07/2017.

REFERENCES

[1] Sprawls P. Physical Principles of Medical Imaging. *Radiology*, 1995; **200**(2): 504. DOI: https://doi.org/10.1148/radiology.200.2.504.

[2] Johns HE, Cunningham JR. *The Physics of Radiology*. 4th ed. Springfield, IL: Charles C Thomas Publisher; 1983.

[3] Hohara S and Nohtomi A. *Neutron Radiography.* Osaka: Atomic Energy Research Institute, Kinki University; 1895.

[4] Eldin MTA. *Neutron Radiography*. Alexandria: Alexandria University; 2011.

[5] Dowsett D, Kenny PA, and Johnston RE. *The Physics of Diagnostic Imaging*. Florida: CRC Press; 2006.

[6] Curry TS, Dowdey JE, and Murry RC. *Cristensen's physics of diagnostic radiology*. 4th edition. Philadelphia: Lippincott Williams & Wilkins; 1990.

[7] Rakhshan V. Image Resolution in the Digital Era: Notion and Clinical Implications. *Journal of Dentistry Shiraz University of Medical Sciences*. 2014; **15**(4): 153-155. Available from: https://dentjods.sums.ac.ir/article_41607.html.

[8] Kondo Y, Han XH, and Chen YW. Two-step Learning Based Super Resolution and Its Application to 3D Medical Volumes. *Proceedings of IEEE 4th Global Conference on Consumer Electronics (GCCE)*. Osaka. 2015; 326-327. DOI: https://doi.org/10.1109/GCCE.2015.7398738.

[9] Hong W, Chen W, and Zhang R. The Application of Neural Network in the Technology of Image Processing. *Proceedings of the International MultiConference of Engineers and Computer Scientists.* Hongkong. 2009; 195-199. Available from: http://www.iaeng.org/publication/IMECS2009/IMECS2009_pp195-199.pdf.

[10] Tang X, Han C, and Liu X. Super-Resolution X-Ray Luminescence Optical Tomography Imaging. *Proceeding of SPIE 11190, Optics in HealthCare and Biomedical Optics IX.* Hangzhou, China. 2019; 111902M. DOI: https://doi.org/10.1117/12.2537540.

[11] Mandal S, Greenblatt AB, and An J. Imaging Intelligence: AI Is Transforming Medical Imaging Across the Imaging Spectrum. *IEEE Pulse*. 2018; **9**(5): 16-24. DOI: https://doi.org/10.1109/MPUL.2018.2857226.

[12] Reddy KSN, Vikram BR, Rao LK, and Reddy BS. Image Compression and Reconstruction Using a New Approach by Artificial Neural Network. *International Journal of Image Processing (IJIP).* 2012; **6**(2): 68-85. Available from: http://www.cscjournals.org/library/manuscriptinfo.php?mc=IJIP-517.

[13] Isaac N. *Handbook of Medical Image Processing and Analysis*. 2nd Edition. Amsterdam: Elsevier; 2009.

[14] Baucher S and Meyer F. *The Morphological Approach to Segmentation the Watershed Transformation*. France: Centre de Morphologie Mathématique Ecole des Mines de Paris. 1993; 433-481. Available from: http://www.cmm.mines-paristech.fr/~beucher/publi/SB_watershed.pdf.

[15] Talele K, Shirsat A, Uplenchwar T, and Tuckley K. Facial expression recognition using general regression neural networks. *Proceedings of IEEE Bombay Section Symposium (IBSS)*. Baramati. 2016; 1-6. DOI: https://doi.org/10.1109/IBSS.2016.7940203.

[16] Umehara K, Ota J, Ishimaru N, Ohno S, Okamoto K, Suzuki T, Shirai N, and Ishida T. Super-resolution convolutional neural network for the improvement of the image quality of magnified images in chest radiographs. *Proceeding of SPIE 10133, Medical Imaging*. Orlando, Florida. 2017; 101331P. DOI: https://doi.org/10.1117/12.2249969.

[17] Mokhtari M, Daneshmand PG, and Rabbani H. Optical Coherence Tomography Image Reconstruction Using Morphological Component Analysis. *Proceedings of 41st Annual International Conference of the IEEE Engineering in Medicine and Biology Society (EMBC)*. Berlin, Germany. 2019; 5601-5604. DOI: https://doi.org/10.1109/EMBC.2019.8857782.

[18] Yu H, Liu D, Shi H, Yu H, Wang Z, Cross B, Bramler M, and Huang TS. Computed Tomography Super-Resolution Using Convolutional Neural Networks. *Proceedings of IEEE International Conference on Image Processing (ICIP)*. Beijing. 2017; 3944-3948. DOI: https://doi.org/10.1109/ICIP.2017.8297022.

[19] Chen Y, Guan H, Hagen CK, Olivo A, Anastasio MA. A Joint-Reconstruction Approach for Single-Shot Edge Illumination X-Ray Phase-Contrast Tomography. *Proceedings of SPIE 10132, Medical Imaging 2017*: *Physics of Medical Imaging*. Florida. 2017; 1013217. DOI: https://doi.org/10.1117/12.2255545.

[20] Schmidt TG, Barber RF, and Sidky EY. Spectral CT Metal Artifact Reduction with An Optimization-Based Reconstruction Algorithm. *Proceedings of SPIE 10132, Medical Imaging: Physics of Medical Imaging*. Florida. 2017; 101321B. DOI: https://doi.org/10.1117/12.2249079.

[21] Rashmi, Kumar M, and Saxena R. Algorithm and Technique on Various Edge Detection: A Survey. *Signal and Image Processing: An International Journal (SIPIJ)*. 2013; **4**(3): 65–75. DOI: http://dx.doi.org/10.5121/sipij.2013.4306.

[22] Alilou VK and Yaghmaee F. Application of GRNN Neural Network in Non-Texture Image Inpainting and Restoration. *Pattern Recognition Letters*. 2015; **62**: 24-31. DOI: https://doi.org/10.1016/j.patrec.2015.04.020.

[23] Panda SS, Prasad MSRS, Prasad MNM, and Naidu SKVR. Image Compression Using Back Propagation Neural Network. *International Journal of Engineering Science & Advanced Technology*. 2012; **2**(1): 74-78. Available from: https://www.ijesat.org/Volumes/2012_Vol_02_Iss_01/IJESAT_2012_02_01_12.pdf.

[24] Al-Mahasneh AJ, Anavatti S, Garratt M, and Pratama M. Applications of General Regression Neural Networks in Dynamic Systems. *IntechOpen*; 2018. DOI: https://doi.org/10.5772/intechopen.80258.

[25] Bej G, Akui A, Pal A, Dey T, Chauduri A, Alam S, Khandaii R, and Bhattacharyya N. X-Ray Imaging and General Regression Neural Network (GRNN) for Estimation of Silk Content in Cocoons. *PerMIn '15: Proceedings of the 2nd International Conference on Perception and Machine Intelligence*. Department of Science and Technology, Government of India. 2015; 71–76. DOI**:** https://doi.org/10.1145/2708463.2709048.

[26] Asad B, Zhi-jiang D, Li-ning S, Reza K, and Fereidoun MA. Fast 3D reconstruction of Ultrasonic Images Based on Generalized Regression Neural Network. *World Congress on Medical Physics and Biomedical Engineering IFMBE Proceedings* Vol 14. Berlin. 2006; 3117-3120. DOI: https://doi.org/10.1007/978-3-540-36841-0_787.

[27] Kumar B, Sinha GR, and Thakur K. Quality Assessment of Compressed MR Medical Images using General Regression Neural Network. *International Journal of Pure & Applied Sciences & Technology*. 2011; **7**(2): 158-169. Available from: https://www.researchgate.net/profile/Professor_G_Sinha/publication/302953762_Quality_assessment_of_compressed_MR_medical_images_using_general_regression_neural_network/links/58d4a593aca2727e5e9af371/Quality-assessment-of-compressed-MR-medical-images-using-general-regression-neural-network.pdf.

[28] Navega D, Coelho JDO, Cunha E, and Curate F. DXAGE: A New Method for Age at Death Estimation Based on Femoral Bone Mineral Density and Artificial Neural Networks. *Journal of Forensic Sciences*. 2018; **63**(2): 497-503. DOI: https://doi.org/10.1111/1556-4029.13582.

[29] Meschino G, Moler EG, and Passoni LI. Semiautomated Segmentation of Bone Marrow Biopsies Images Based on Texture Features and Generalized Regression Neural Networks. *X Congreso Argentino de Ciencias de la Computación*. National University La Plata, Buinos Aires; 2004. Available from: http://sedici.unlp.edu.ar/handle/10915/22371.

[30] Sankara Rao P and Kumar RK. An Improved Neural Network to Estimate Effort of Medical Imaging Software Development. *Journal of Medical Imaging and Health Informatics*. 2016; **6**(8): 1977-1982. DOI**:** https://doi.org/10.1166/jmihi.2016.1960.